Available online at www.sciencedirect.com
ScienceDirect
International Journal of Thermal Sciences 48 (2009) 547–553
International Journal of Thermal Sciences
www.elsevier.com/locate/ijts

Approximate analytical solution for one-dimensional tissue freezing around cylindrical cryoprobes

Latif M. Jiji *, Peter Ganatos

Department of Mechanical Engineering, The City College of the City University of New York, New York, NY 10031, USA

Received 20 December 2007; received in revised form 28 April 2008; accepted 29 April 2008

Available online 2 June 2008

Abstract

An approximate analytical solution for the temperature distribution and interface motion is determined for the freezing of blood-perfused tissue around a cylindrical cryoprobe. The solution is based on an improved quasi-steady model in which assumed temperature profiles in the frozen and unfrozen tissue are used to determine the interface motion. The approximate solution satisfies all temperature boundary conditions as well as the transient heat equations at the interface. Due to blood perfusion in the unfrozen tissue, a steady state is reached where the interface becomes stationary. The solution converges to the exact steady state interface location. Improvement over the quasi-steady solution and the accuracy of the present theory are verified by comparison with numerical solutions for the limiting case of zero blood perfusion and metabolic heat production. Results show that a typical quasi-steady error of 73% is reduced to 8% using the present theory. Parametric charts are presented to evaluate the effect of the governing parameters on interface location.

Keywords: Tissue freezing; Cryoprobes; Phase change; Improved quasi-steady; Moving boundary

1. Introduction

A major interest in the application of cryoprobes is the determination of the moving frozen front position. Problems involving phase change are encountered in a wide range of applications such as food preservation, energy storage and geology. Although phase change problems have been analyzed during the last century and a half, there are very few exact solutions [1–4]. The mathematical difficulty is traced to the non-linearity of the interface energy balance condition. Because of the added complexity of blood perfusion, metabolic heat production and vascular architecture in tissue freezing, solutions are commonly based on numerical techniques [5–10] or approximate analytical methods [11–16]. A common approximation is based on the quasi-steady assumption [16–20]. In this model the mathematical problem is vastly simplified by neglecting the transient terms in the governing heat equations. The Stefan number, which is the ratio of sensible to latent heat, is used as a criterion for the applicability of the quasi-steady model. Results based on this model are valid for small Stefan numbers compared to unity. Although the quasi-steady model is useful in providing approximate solutions, it has severe inherent disadvantages since it does not account for the effect of Stefan number and thermal diffusivity. Consequently, the method is not useful for performing comprehensive parametric studies. In a recently published paper, Lin and Zheng [20] partially address this issue by approximately accounting for the sensible heat to improve quasi-steady solutions to freezing of non-biological medium. Their solution is based on an assumed temperature profile in the frozen region. The assumed profile makes use of Stefan's exact Cartesian solution to freezing of a semi-infinite non-biological material. They applied this approach to three one-dimensional problems involving planar, cylindrical and spherical geometries. In all cases the non-biological material is assumed to be initially at the fusion temperature. Based on this assumption the unfrozen region plays no role in the solution. Comparison with exact results showed excellent improvement over the quasi-steady solutions.

* Corresponding author. Tel.: +1 212 650 5228; fax: +1 212 650 8013.
E-mail addresses: jiji@ccny.cuny.edu (L.M. Jiji), ganatos@ccny.cuny.edu (P. Ganatos).

1290-0729/$ – see front matter
doi:10.1016/j.ijthermalsci.2008.04.003

Nomenclature

c_s	specific heat
k	thermal conductivity of unfrozen tissue
$\mathcal{L}$	latent heat of fusion
q_m	volumetric metabolic heat production rate
r	cylindrical coordinate
r_o	radius of cylindrical probe
St	Stefan number, defined in (3)
t	time
T	temperature, unfrozen tissue
w_b	volumetric blood perfusion rate per unit tissue volume

Subscript

$a0$	arterial blood supply temperature
b	blood
f	fusion
i	interface
in	initial
o	surface
s	solid phase

Superscript

n	exponent in the assumed unfrozen tissue temperature

Greek

α	thermal diffusivity
β	blood perfusion parameter, defined in (3)
γ	metabolic heat production parameter, defined in (3)
κ	conductivity-temperature ratio parameter, defined in (11)
θ	dimensionless temperature, defined in (3)
ρ_b	blood density
τ	dimensionless time, defined in (3)
ξ	dimensionless distance, defined in (3)
$\xi_i(\infty)$	dimensionless steady state interface position

In this paper we examine freezing of a blood-perfused tissue around a cylindrical probe. The method used in the analysis of planar and spherical probes [15] is extended to tissue freezing around cylindrical probes. Tissue heat transfer analysis requires the use of an appropriate bioheat equation. One of the earliest equations was formulated and applied by Pennes in 1948 [21]. In this equation blood effect is modeled as a local, tissue temperature-dependent, heat source or sink. Because of the simplicity and reasonable accuracy under certain conditions, Pennes' bioheat equation has been extensively used in heat transfer analysis of biological tissues under thawing and freezing conditions. Although the method of Lin and Zheng cannot be applied to this problem, a different approach is introduced to improve the accuracy of the quasi-steady approximation in both the frozen and unfrozen regions. Solutions to the temperature distribution and interface motion account for blood perfusion, metabolic heat generation, arterial supply temperature, Stefan number and thermal diffusivity effects.

2. Analysis

2.1. Problem statement and formulation

We consider one-dimensional freezing of tissue around a cylindrical cryosurgical probe of radius r_o shown in Fig. 1. The tissue is assumed to undergo phase transformation at a discrete fusion temperature T_f. The probe is embedded in an infinite tissue initially at uniform temperature T_{in}. The surface of the probe is suddenly maintained at uniform temperature $T_o < T_f$. Metabolic heat is generated throughout the unfrozen tissue at a constant volumetric rate q_m. Blood at the arterial temperature T_{a0} is supplied to the tissue at a uniform volumetric rate per unit tissue volume, w_b. Tissue freezing commences instantaneously at $r = r_o$ and propagates outwards in the radial direction.

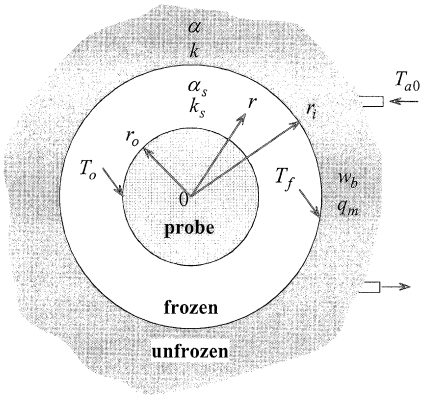

Fig. 1. Cross section of cylindrical probe.

2.2. Governing equations

Since this is a two-phase problem, an appropriate heat equation must be formulated for each phase. Noting that metabolic activity and blood perfusion cease in frozen tissue, the classical heat conduction equation is applicable in this region. For the unfrozen tissue we use Pennes' bioheat equation [21]. Expressed in dimensionless form, the governing heat equations are given by

$$\frac{1}{\xi}\frac{\partial}{\partial\xi}\left[\xi\frac{\partial\theta_s}{\partial\xi}\right] = St\frac{\partial\theta_s}{\partial\tau}, \quad 1 \leqslant \xi \leqslant \xi_i \tag{1}$$

and

$$\frac{1}{\xi}\frac{\partial}{\partial\xi}\left[\xi\frac{\partial\theta}{\partial\xi}\right] - \beta\theta - \gamma = St\frac{\alpha_s}{\alpha}\frac{\partial\theta}{\partial\tau}, \quad \xi \geqslant \xi_i \tag{2}$$

The subscript s refers to the solid phase (frozen tissue), α is thermal diffusivity and *St* is the *Stefan number*. The dimensionless variables and parameters are defined as

$$\theta_s = \frac{T_s - T_o}{T_f - T_o}, \qquad \theta = \frac{T - T_{a0}}{T_f - T_{a0}}$$

$$\xi = \frac{r}{r_o}, \qquad \tau = St\frac{\alpha_s}{r_o^2}t$$

$$\beta = \frac{\rho_b c_b w_b r_o^2}{k}, \qquad \gamma = \frac{q_m r_o^2}{k(T_{a0} - T_f)}$$

$$St = \frac{c_s(T_f - T_o)}{\mathcal{L}} \tag{3}$$

Subscript b refers to blood, c is specific heat and $\mathcal{L}$ is the latent heat of fusion.

2.3. Boundary and initial conditions

The dimensionless form of the boundary conditions are

$$\theta_s(1,\tau) = 0 \tag{4}$$

$$\theta_s(\xi_i,\tau) = 1 \tag{5}$$

$$\theta(\xi_i,\tau) = 1 \tag{6}$$

$$\theta(\infty,\tau) = -\gamma/\beta \tag{7}$$

The initial conditions are

$$\theta(\xi,0) = -\gamma/\beta \tag{8}$$

$$\xi_i(0) = 1 \tag{9}$$

Conservation of energy at the interface gives

$$\frac{d\xi_i}{d\tau} = \frac{\partial\theta_s(\xi_i,\tau)}{\partial\xi} + \kappa\frac{\partial\theta(\xi_i,\tau)}{\partial\xi} \tag{10}$$

where κ is defined as

$$\kappa = \frac{k(T_{a0} - T_f)}{k_s(T_f - T_o)} \tag{11}$$

Examination of the dimensionless equations shows that the problem is governed by five parameters: diffusivity ratio α_s/α, blood perfusion β, metabolic heat production γ, conductivity-temperature ratio κ, and Stefan number St.

2.4. Simplified model: quasi-steady approximation [16]

From the definition of the Stefan number in (3), it follows that for a small Stefan number, interface motion is dominated by the latent heat. Consequently, the interface moves slowly such that the instantaneous temperature distribution corresponds to the steady state. Based on this argument the transient terms in (1) and (2) are neglected. The solution to the resulting equations, subject to boundary conditions (4)–(7), is detailed in the literature [16]. The temperature distribution in the frozen and unfrozen regions for this model is given by

$$\theta_s = \frac{\ln\xi}{\ln\xi_i} \tag{12}$$

and

$$\theta = \left(1 + \frac{\gamma}{\beta}\right)\frac{K_0(\sqrt{\beta}\xi)}{K_0(\sqrt{\beta}\xi_i)} - \frac{\gamma}{\beta} \tag{13}$$

Substituting (12) and (13) into (10) gives

$$\frac{d\xi_i}{d\tau} = \frac{1}{\xi_i\ln\xi_i} - \kappa\sqrt{\beta}\left(1 + \frac{\gamma}{\beta}\right)\frac{K_1(\sqrt{\beta}\xi_i)}{K_0(\sqrt{\beta}\xi_i)} \tag{14}$$

Numerical integration of (14), using initial condition (9), gives the interface location $\xi_i(\tau)$. It is instructive to note that the solution is independent of Stefan number and the diffusivity parameter α_s/α. This is typical of all quasi-steady solutions.

2.5. Improved quasi-steady solution

We seek to improve the accuracy of the quasi-steady solution, eliminate its limitation to small Stefan's numbers and include the effect the diffusivity parameter α_s/α. Since Stefan solution does not apply to metabolic heat production in a blood perfused cylindrical tissue, the method of Lin and Zheng cannot be applied to this case. A unique feature of the tissue problem is the existence of a steady state condition corresponding to $\tau \to \infty$. This is not the case with the Stefan and Neumann problems. The exact steady state tissue temperature distribution and interface location can be easily determined.

To improve the quasi-steady solution of the tissue problem, a new approach is developed that does not require the use of exact solutions to related problems. Rather than solving the quasi-steady equations, appropriate temperature profiles are assumed for the frozen and unfrozen phases. The assumed profiles satisfy all boundary conditions as well as the two transient heat equations, (1) and (2), at the moving interface. In addition, the assumed profiles insure that the steady state interface location converges to the exact solution.

2.5.1. Assumed temperature profiles

The following profile is assumed in the frozen finite tissue

$$\theta_s(\xi,\tau) = 1 + a_1\left[\frac{\xi}{\xi_i} - 1\right] + a_2\left[\frac{\xi}{\xi_i} - 1\right]^2 \tag{15}$$

The assumed profile in the semi-infinite unfrozen tissue is an exponential of the form

$$\theta(\xi_i,\tau) = b_0 + b_1\exp\left[-b_2\frac{\xi^n}{\xi_i^n}\right] \tag{16}$$

These profiles are dependent on seven unknown factors: $a_0, a_1, a_2, b_0, b_1, b_2$ and n. The exponent n is assumed constant and the remaining coefficients may be constants or functions of $\xi_i(\tau)$. In addition to the four boundary conditions on θ_s and θ, three additional conditions are needed. Two conditions are formulated based on the invariance of interface temperature, the satisfaction of heat equations (1) and (2) at the interface, and conservation of energy (10) at the interface $\xi = \xi_i$. Since interface temperature T_f remains constant at all times, it follows that

$$d\theta_s(\xi_i,\tau) = \frac{\partial\theta_s(\xi_i,\tau)}{\partial\xi}d\xi_i + \frac{\partial\theta_s(\xi_i,\tau)}{\partial\tau}d\tau = 0$$

Solving the above for $\frac{d\xi_i}{d\tau}$ and using (1) to eliminate $\frac{\partial\theta_s(\xi_i,\tau)}{\partial\tau}$ yields

$$\frac{d\xi_i}{d\tau} = -\frac{\frac{\partial^2\theta_s(\xi_i,\tau)}{\partial\xi^2} + \frac{1}{\xi_i}\frac{\partial\theta_s(\xi_i,\tau)}{\partial\xi}}{St\frac{\partial\theta_s(\xi_i,\tau)}{\partial\xi}} \tag{17}$$

Substituting (17) into (10) gives

$$\left[\frac{\partial\theta_s(\xi_i,\tau)}{\partial\xi}\right]^2+\kappa\frac{\partial\theta_s(\xi_i,\tau)}{\partial\xi}\frac{\partial\theta(\xi_i,\tau)}{\partial\xi}+\frac{1}{St}\left[\frac{\partial^2\theta_s(\xi_i,\tau)}{\partial\xi^2}+\frac{1}{\xi_i}\frac{\partial\theta_s(\xi_i,\tau)}{\partial\xi}\right]=0 \tag{18}$$

Similarly, constancy of the temperature of the unfrozen region at the interface, heat equation (2) and interface energy equation (10) give

$$\frac{\partial\theta_s(\xi_i,\tau)}{\partial\xi}\frac{\partial\theta(\xi_i,\tau)}{\partial\xi}+\kappa\left[\frac{\partial\theta(\xi_i,\tau)}{\partial\xi}\right]^2+\frac{1}{St}\frac{\alpha}{\alpha_s}\left[\frac{\partial^2\theta(\xi_i,\tau)}{\partial\xi^2}+\frac{1}{\xi_i}\frac{\partial\theta(\xi_i,\tau)}{\partial\xi}-\beta-\gamma\right]=0 \tag{19}$$

A third condition is based on the interface steady state solution $\xi_i=\xi_i(\infty)$ obtained by setting $d\xi_i/dt=0$ in (10) to obtain

$$\frac{\partial\theta_s(\xi_i,\infty)}{\partial\xi}+\kappa\frac{\partial\theta(\xi_i,\infty)}{\partial\xi}=0 \tag{20}$$

Application of boundary conditions (4)–(7) gives

$$a_0=1,\qquad a_2=-\frac{1+a_1(\xi_l^{-1}-1)}{(\xi_i^{-1}-1)^2}$$

$$b_0=-\frac{\gamma}{\beta},\qquad b_1=\left[1+\frac{\gamma}{\beta}\right]\exp b_2$$

The assumed profiles (15) and (16) become

$$\theta_s(\xi,\tau)=1+a_1\left(\xi_i^{-1}\xi-1\right)-\left[1+a_1\left(\xi_i^{-1}-1\right)\right]\frac{(\xi-\xi_i)^2}{(1-\xi_i)^2} \tag{21}$$

and

$$\theta(\xi,\tau)=-\frac{\gamma}{\beta}+\frac{\gamma+\beta}{\beta}\exp\left(b_2-b_2\xi_i^{-n}\xi^n\right) \tag{22}$$

Application of (21) and (22) to conditions (18)–(20) gives three equations for a_1, b_2 and n:

$$a_1^2-\kappa\left[1+\frac{\gamma}{\beta}\right]na_1b_2+\frac{1}{St}\left[a_1-2\frac{1+a_1(\xi_i^{-1}-1)}{(\xi_i^{-1}-1)^2}\right]=0 \tag{23}$$

$$a_1-\kappa\left[1+\frac{\gamma}{\beta}\right]nb_2+\frac{1}{St}\frac{\alpha}{\alpha_s}\left[n(1-b_2)+\frac{\beta\xi_i^2}{nb_2}\right]=0 \tag{24}$$

and

$$n=\frac{a_1(\infty)}{\kappa[1+\gamma/\beta]b_2(\infty)} \tag{25}$$

Evaluating (23) and (24) at $\tau=\infty$ and combining the resulting equations with (25) gives three equations for $a_1(\infty), b_2(\infty)$ and n. The solution to the three equations gives the constant n in terms of steady state interface location $\xi_i(\infty)$

$$n=\frac{2}{\kappa[1+\gamma/\beta]}\frac{1}{[\xi_i^{-1}(\infty)-1][\xi_i^{-1}(\infty)-3]}-\frac{\beta\kappa}{2}\left[1+\frac{\gamma}{\beta}\right]\xi_i^2(\infty)\left[\xi_i^{-1}(\infty)-1\right]\left[\xi_i^{-1}(\infty)-3\right] \tag{26}$$

The exact steady state interface location $\xi_i(\infty)$ is determined by setting $d\xi_i/dt=0$ in (14)

$$\frac{1}{\xi_i(\infty)[\ln\xi_i(\infty)]}\frac{K_0[\sqrt{\beta}\xi_i(\infty)]}{K_1[\sqrt{\beta}\xi_i(\infty)]}=\kappa\sqrt{\beta}\left(1+\frac{\gamma}{\beta}\right). \tag{27}$$

The solution to this transcendental equation gives $\xi_i(\infty)$.

With n determined, MATLAB is used to solve (23) and (24) for a_1 and b_2 as functions of ξ_i.

2.5.2. Interface motion

To determine the interface location, assumed profiles (21) and (22) are substituted into interface energy equation (10)

$$\frac{d\xi_i}{d\tau}=\frac{a_1}{\xi_i}-\kappa\left[1+\frac{\gamma}{\beta}\right]\frac{nb_2}{\xi_i} \tag{28}$$

Solutions to $a_1(\xi_i)$ and $b_2(\xi_i)$ are substituted into (28) and the resulting equation is integrated numerically using initial condition (9) to give the transient solution to the interface location.

3. Results and discussion

3.1. Solution accuracy

To evaluate the accuracy of the present theory, comparison is made with the limiting case of freezing of non-biological material with no blood perfusion or metabolic heat; $\beta=\gamma=0$. A numerical solution to this problem is available in the literature [22]. It should be noted that this special case has no steady state interface solution. This is also true of the analogous Neumann's problem. This has an important consequence on the assumed temperature profile in (16) where the exponent n is introduced to satisfy the steady state interface condition. Since the limiting case of $\beta=\gamma=0$ has no steady state, we set $n=1$. Thus the improved quasi-steady state solution to this limiting case is determined by setting $\beta=\gamma=0$ and $n=1$ in (23) and (24) to obtain

$$a_1^2-\kappa a_1b_2+\frac{1}{St}\left[a_1-2\frac{1+a_1(\xi_i^{-1}-1)}{(\xi_i^{-1}-1)^2}\right]=0 \tag{29}$$

and

$$a_1-\kappa b_2+\frac{1}{St}\frac{\alpha}{\alpha_s}(1-b_2)=0 \tag{30}$$

Eqs. (29) and (30) can be solved analytically for $a_1(\xi_i)$ and $b_2(\xi_i)$. The interface location ξ_i is determined from (28), which simplifies to

$$\frac{d\xi_i}{d\tau}=\frac{a_1}{\xi_i}-\kappa\frac{b_2}{\xi_i} \tag{31}$$

Numerical integration of (31) gives the improved quasi-steady interface location for this limiting case. Note that in the definition of κ in (11) the blood supply temperature T_{a0} is replaced by the initial temperature T_i.

The improved solution of the present theory is compared with the numerical solution in Fig. 2. Also shown is the quasi-steady solution. The interface location ξ_i is plotted as a function

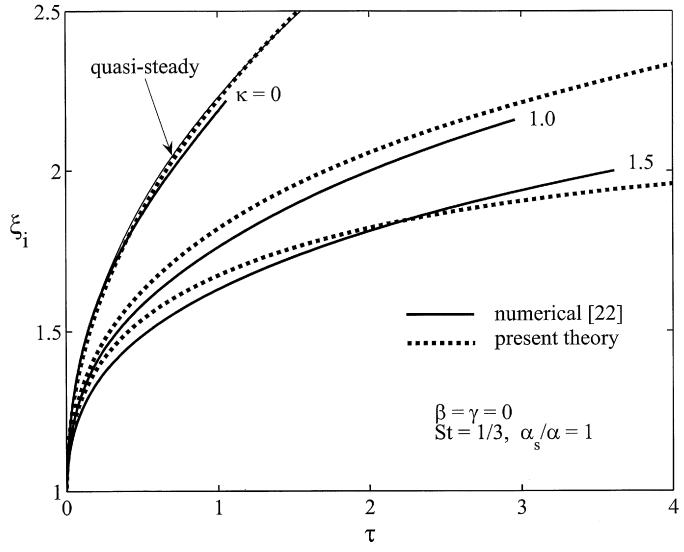

Fig. 2. Comparison of $\xi(\tau)$ with the numerical solution, $\beta = \gamma = 0$, $\alpha/\alpha_s = 1$, $St = 1/3$.

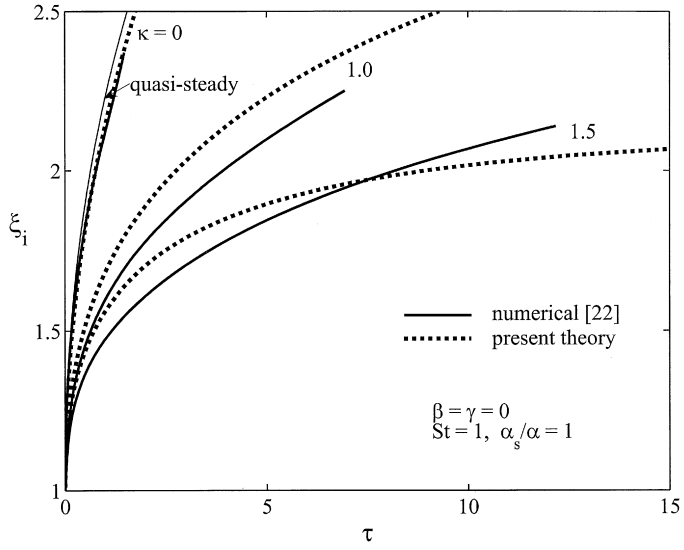

Fig. 3. Comparison of $\xi(\tau)$ with the numerical solution, $\beta = \gamma = 0$, $\alpha/\alpha_s = 1$, $St = 1$.

of time for three values of the parameter κ for $\alpha_s/\alpha = 1$ and $St = 1/3$. The limiting case of $\kappa = 0$ corresponds to a material which is initially at the freezing temperature. The error of the present theory at $\tau = 1, 2$, and 3 for $\kappa = 1.0$ is 3.3%, 2.9% and 2.2%, respectively. The corresponding error of the quasi-steady solution is 26.5%, 34.2% and 39.3%. Since the quasi-steady solution for this case is independent of the parameter κ, its error increases with increasing κ. For example, for $\kappa = 1.5$ the errors become 36.6%, 48% and 55.7%. On the other hand, the error of the present theory remains below 3%. Fig. 3 shows the effect of increasing the Stefan number to 1.0. Since the quasi-steady solution is independent of St, its accuracy deteriorates with increasing Stefan number. For $\kappa = 1.0$ and $\tau = 3$ the error is 58%. The corresponding error of the present theory is 6.3%. The parameter α_s/α reflects the contribution of the unfrozen tissue to interface motion. Fig. 4 gives the interface location for

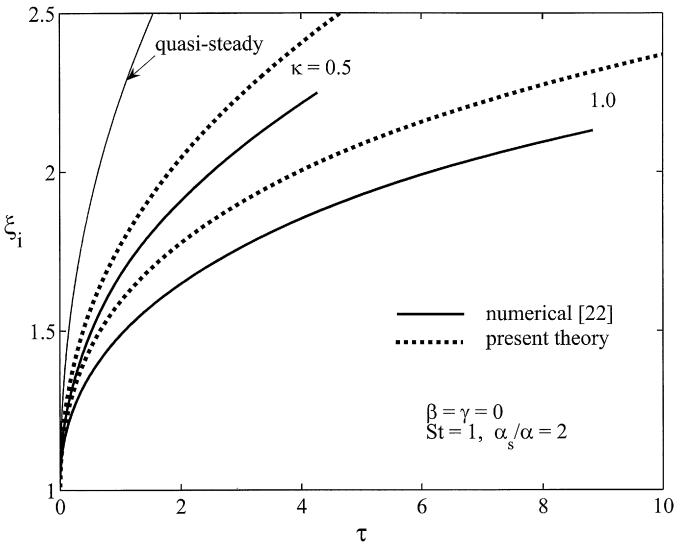

Fig. 4. Comparison of $\xi(\tau)$ with the numerical solution, $\beta = \gamma = 0$, $\alpha/\alpha_s = 2$, $St = 1$.

$\alpha_s/\alpha = 2$. At $\kappa = 1.0$, $St = 1.0$ and $\tau = 3$ the quasi-steady error is 71% while the error of the present theory is 7.7%.

It should be emphasized that comparison with the numerical solution is for the special case of $\beta = \gamma = 0$. As was pointed out, this case has no steady state and thus, unlike application to tissue freezing, convergence to the exact solution at large time is not assured. In addition, typical values of κ for cryoprobes are of order 0.15. This is much lower than the values used in the numerical solution cases. Thus the conditions of the accuracy test cases used in Figs. 2–4 contribute to larger errors not likely to be encountered when the present theory is applied to tissue freezing with blood perfusion and metabolic heat production.

3.2. Parametric studies

Having established the significant improvement of the present theory over the quasi-steady model, we proceed to carry out parametric study of the interface location. Tissue temperature and interface location are governed by five parameters: α_s/α, β, γ, κ, and the Stefan number St. However, it is instructive to examine the relationship between St and κ. From their definitions in (3) and (11) we obtain

$$\kappa = \frac{k}{k_s}\frac{c_s(T_{a0} - T_f)}{\mathcal{L}}\frac{1}{St} \tag{32}$$

Except for T_{a0}, all quantities in the coefficient of St in (32) are tissue properties. However, since the variation in blood supply temperature T_{a0} is relatively small, the effect of κ will not be examined as an independent parameter.

Figs. 5–8 examine the effects of blood perfusion β, metabolic heat γ, Stefan number St and diffusivity ratio α_s/α on the interface motion. Characteristic of these cases is the existence of steady state interface location. Both quasi-steady and present theory converge to the exact interface condition. For all cases considered, increasing β results in a decrease in the steady state interface location $\xi_i(\infty)$ as well as the time needed to approach steady state. This follows from the fact that blood energy supply

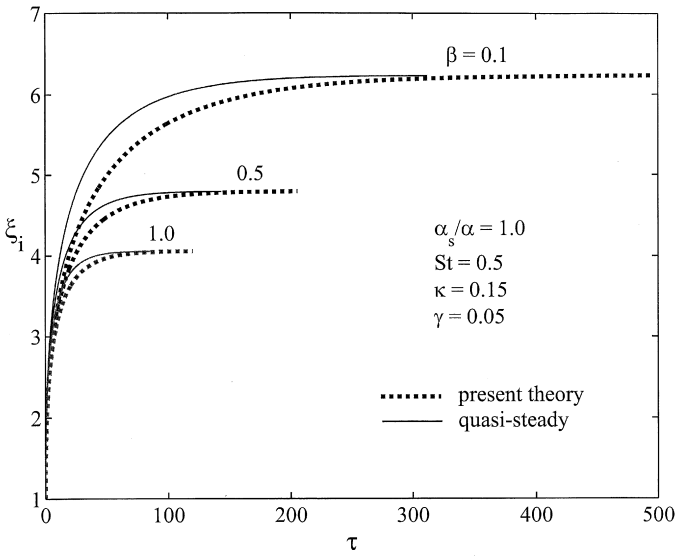

Fig. 5. Effect of β on interface location $\xi(\tau)$ for $\alpha/\alpha_s = 1$, $\gamma = 0.05$, $\kappa = 0.15$, $St = 0.5$.

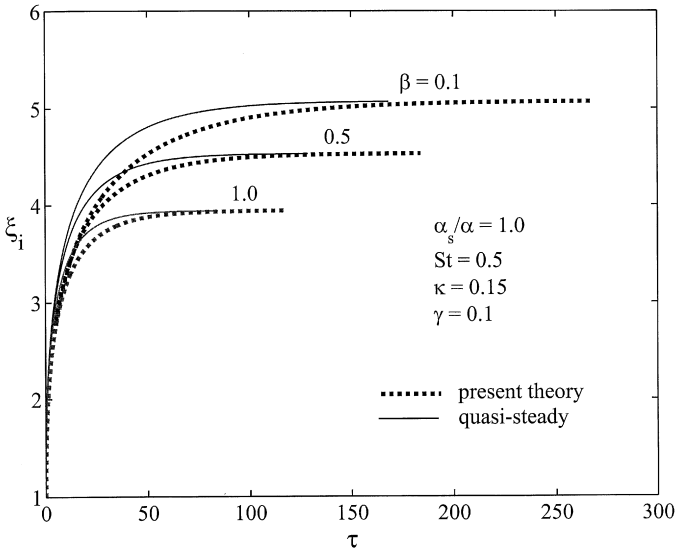

Fig. 6. Effect of β on interface location $\xi(\tau)$ for $\alpha/\alpha_s = 1$, $\gamma = 0.1$, $\kappa = 0.15$, $St = 0.5$.

in the unfrozen tissue slows down interface motion and prevents it from penetrating further into the tissue. Increasing γ has the same effect, as indicated when Fig. 5 is compared with Fig. 6. However, neither the Stefan number St nor the diffusivity ratio α_s/α has an effect on $\xi_i(\infty)$. On the other hand, κ does, as indicated in (27). From the definition of κ in (11), a decrease in κ can come about by an increase in the conductivity of the frozen region k_s. This results in an increase in heat removal from the interface and a corresponding increase in its velocity and steady state location $\xi_i(\infty)$. This is verified when Fig. 5 is compared with Fig. 7. The effect of α_s/α on interface location is not very significant. This is evident when Fig. 7 ($\alpha_s/\alpha = 1$) is compared with Fig. 8 ($\alpha_s/\alpha = 10$). For example, interface location ξ_i at $\tau = 2000$ decreases by 9.4% when α_s/α is increased by a factor of 10.

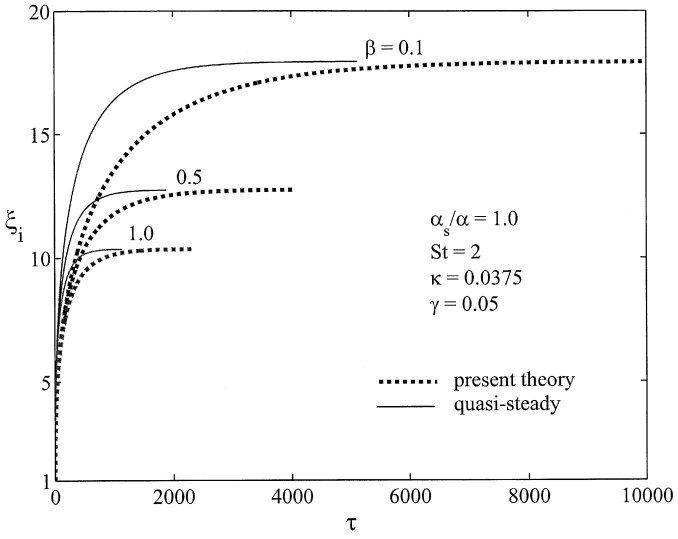

Fig. 7. Effect of β on interface location $\xi(\tau)$ for $\alpha/\alpha_s = 1$, $\gamma = 0.05$, $\kappa = 0.0375$, $St = 2$.

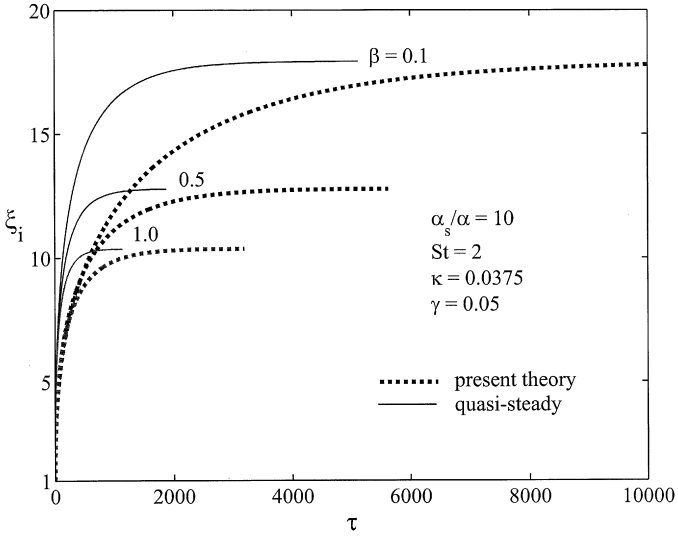

Fig. 8. Effect of β on interface location $\xi(\tau)$ for $\alpha/\alpha_s = 10$, $\gamma = 0.05$, $\kappa = 0.0375$, $St = 2$.

To compare the quasi-steady solution with the present theory, we define the percent difference between the two solutions, δ, as

$$\delta = \frac{(\xi_i)_{\text{quasi-steady}} - (\xi_i)_{\text{present}}}{(\xi_i)_{\text{present}}} 100 \tag{33}$$

Examination of Figs. 5–8 shows that δ depends on the parameters α_s/α, β, γ, κ, St and the variable τ. For the values of the parameters considered in Figs. 5–8, the error ranges from negligible to 38%. Results show that δ increases with increasing α_s/α and St. However, it decreases as β and τ are increased.

4. Conclusions

An improved quasi-steady solution for tissue solidification around a cylindrical probe is presented. The solution accounts for blood perfusion and metabolic heat production. The solution

to the temperature distribution in the frozen and unfrozen tissue satisfies all boundary conditions as well as the two heat equations at the interface. Steady state interface location is satisfied exactly. Interface location was found to depend on five parameters: α_s/α, β, γ, κ, and the Stefan number St. The accuracy of the improved solution was evaluated by comparison with the numerical solution to the limiting case of $\beta = \gamma = 0$. Significant improvement over the quasi-steady solution was obtained. For example, a typical quasi-steady error of 73% is reduced to 8% using the present theory. Parametric studies show that β, γ, κ, and the Stefan number St have significant effect on interface location. However, the effect of α_s/α is relatively small even when it is increased by a factor of 10.

References

[1] H.S. Carslaw, J.C. Jaeger, in: Conduction of Heat in Solids, Oxford at the Clarendon Press, 1959, pp. 283–296.

[2] Y. Rabin, A. Shitzer, Combined solutions of the inverse-Stefan problem for successive freezing/thawing in non-ideal biological tissues, J. Biomech. Eng. 119 (1997) 146–152.

[3] Y. Rabin, A. Shitzer, Exact solution to the one-dimensional inverse-Stefan problem in cryosurgical probe, J. Heat Trans. 117 (1995) 425–431.

[4] B. Rubinsky, A. Shitzer, Analysis of Stefan-like problem in a biological tissue around cryosurgical probe, J. Heat Trans. 98 (1976) 514–519.

[5] Z.S. Deng, J. Liu, Modeling multidimensional freezing problems during cryosurgery by dual reciprocity boundary element method, Eng. Anal. Bound. Elem. 28 (2004) 97–108.

[6] Y.T. Zhang, J. Liu, Numerical study on three-region thawing problem during cryosurgical re-warming, Med. Eng. Phys. 24 (2002) 265–277.

[7] Y. Rabin, A. Shitzer, Numerical solution of the multi-dimensional freezing problem during cryosurgery, J. Biomech. Eng. 120 (1998) 32–37.

[8] J.C. Rewcastle, G.A. Sandison, K. Muldrew, J.C. Saliken, B.J. Donnelly, A model for the time dependent three-dimensional thermal distribution within ice balls surrounding multiple cryoprobes, Med. Phys. 28 (2001) 1125–1137.

[9] R.I. Andrushkiw, Mathematical modeling of freezing front propagation in biological tissue, Math. Comp. Model. 13 (1990) 1–9.

[10] A. Weill, A. Shitzer, P. Bar-Yoseph, Finite element analysis of the temperature field around two adjacent cryoprobes, J. Biomech. Eng. 115 (1993) 374–379.

[11] H.M. Budman, A. Shitzer, J. Dayan, Analysis of the inverse problem of freezing and thawing of a binary solution during cryosurgical processes, J. Biomech. Eng. 117 (1995) 192–202.

[12] K.R. Diller, A simple procedure for determining spatial distribution of cooling rates within a specimen during cryopreservation, I. Analysis, J. Eng. Med. 204 (1990) 179–187.

[13] W.J. Song, L.M. Jiji, Peripheral tissue freezing in cryosurgery, Cryobiology 25 (1988) 153–163.

[14] H.M. Budman, A. Shitzer, S. del Giudice, Investigation of temperature field around embedded cryoprobes, J. Biomech. Eng. 108 (1986) 42–48.

[15] L.M. Jiji, P. Ganatos, Freezing of blood perfused tissue: an improved quasi-steady solution, Int. J. Heat Mass Trans., in press.

[16] G.J. Trezek, Thermal analysis for cryosurgery, in: A. Shitzer, R.C. Eberhart (Eds.), Heat Transfer in Medicine and Biology, vol. 2, Plenum Press, New York, 1985, pp. 239–258.

[17] S. Chakraborty, P. Dutta, Analytical solutions for heat transfer during cyclic melting and freezing of a phase change material used in electronic or electrical packaging, J. Electro. Packaging 125 (2003) 126–133.

[18] C.K. Hsieh, M. Leung, Phase change in a cylinder and cylindrical shell heated with an axisymmetric front moving in the axial direction, J. Heat Trans. 123 (2001) 476–485.

[19] T.J. Lu, Thermal management of high power electronics with phase change cooling, Int. J. Heat Mass Trans. 43 (2000) 2245–2256.

[20] S. Lin, J. Zheng, An improved quasi-steady analysis for solving freezing problems in a plate, a cylinder and a sphere, J. Heat Trans. 125 (2003) 1123–1128.

[21] H.H. Pennes, Analysis of tissue and arterial blood temperatures in the resting forearm, J. Appl. Phys. 1 (1948) 93–122.

[22] L.C. Tien, S.W. Churchill, Freezing front motion and heat transfer outside an infinite, isothermal cylinder, AIChE J. 11 (1965) 790–793.